Science of the Total Environment 472 (2014) 1121–1129

Contents lists available at ScienceDirect

Science of the Total Environment

journal homepage: www.elsevier.com/locate/scitotenv

Elemental profiles and signatures of fugitive dusts from Chinese deserts

Rong Zhang [a], Junji Cao [a,*], Yanrong Tang [a], Richard Arimoto [a,1], Zhenxing Shen [b], Feng Wu [a], Yongming Han [a], Gehui Wang [a], Jiaquan Zhang [c], Guohui Li [a]

[a] State Key Laboratory of Loess and Quaternary Geology (SKLLQG), Institute of Earth Environment (IEE), Chinese Academy of Sciences, No. 10 Fenghui South Rd., High-Tech Zone, Xi'an 710075, China
[b] Department of Environmental Science and Engineering, Xi'an Jiaotong University, No. 28 Xianning West Rd., Xi'an 710049, China
[c] Hubei Polytechnic University, No. 16 Guilin North Rd., Huangshi 435003, China

HIGHLIGHTS

- Elemental profiles were supplied for size-separated dust particles from Chinese deserts.
- Na/S, Mg/S, Fe/Al, K/Al etc. ratios were used to differentiate the two desert sources.
- Higher Pb, As, Cd etc. for N than NW implied stronger pollution to northern deserts.

ARTICLE INFO

Article history:
Received 9 August 2013
Received in revised form 3 October 2013
Accepted 2 November 2013
Available online 19 December 2013

Keywords:
Elemental profiles
Chinese deserts
Asian dust
Source signatures

ABSTRACT

Elemental profiles were determined for size-separated fugitive dust particles produced from Chinese desert and gobi soils. Seventeen surface soil samples from six Chinese deserts were collected, composited, resuspended, and sampled through TSP, PM_{10}, and $PM_{2.5}$ inlets onto Teflon® filters, which were analyzed for twenty-six elements. Two major dust sources could be distinguished based on differences in crustal and enriched elements—the northwestern (NW) region (Taklimakan Desert, Xinjiang Gobi, and Anxinan Gobi) and northern (N) region (Ulan Buh Desert, Central Inner Mongolia Desert, and Erenhot Gobi). The N sources showed lower concentrations of mineral elements (Fe, K, Na, Ti, Mn, Cr, and Rb in PM_{10}, and Fe, K, Ti, Mn, Co, and V in $PM_{2.5}$) and higher levels of contaminants (S, Zn, Mo, Cu, Cr, Pb, Cd, and As) than the NW ones, especially in $PM_{2.5}$. Enrichment factors for Cu, Cr, Zn, Pb, As, Mo, and Cd calculated relative to the upper continental crust showed enrichments of one to two orders-of-magnitude, and they were much higher for N sources than NW ones, implying stronger anthropogenic impacts in north China. Aerosol elemental concentrations during dust events at Horqin, Beijing, and Xi'an matched the mass percentages of mineral elements from their presumptive sources better than the alternative ones, validating the differences between the NW and N sources. Additionally, Na/S, Mg/S, Fe/Al, K/Al, Si/Fe, and Na/Al ratios were suggested to differentiate the two dust source regions. The elemental ratios of Ca/Al, K/Al, Fe/Al, and Ti/Fe in the source regions matched those in aerosols collected downwind, and they can be considered as possible source indicators.

1. Introduction

Mineral aerosol has become of increasing interest to earth scientists because of its importance for climate and environmental change (Cziczo et al., 2013; Uno et al., 2009). A billion or more tons of mineral dusts are produced globally with major sources in the Sahara and Sahel in North Africa, Asia, southwestern North America, and the Lake Eyre Basin in Australia (Prospero et al., 2002; Lawrence and Neff, 2009; Radhi et al., 2010). Mineral dust emitted from the Chinese deserts is one of the major components of the ambient aerosol over East Asia, including China, Korea, and Japan, especially in spring (Cao et al., 2003; Kim et al., 2003; Chio et al., 2004; Cao et al., 2012).

About half of the dust produced in Asia is transported thousands of kilometers over the North Pacific and even as far as North America (Zhang et al., 1997); this Asian dust degrades air quality, plays important roles in climate change, and impacts biogeochemical cycles (Martin and Fitzwater, 1988; Zhuang et al, 1992; Cao et al., 2003). It has been proposed that the Chinese deserts can be divided into different regions based on their geology and geomorphology, and these differences affect the characteristics of the dust particles they produce (Zhang et al., 1996). In the historical period, the dust sources for the Chinese Loess Plateau shifted between southern Mongolia during cold periods and northern China during warm periods (Sun et al., 2008). Information on the composition of the mineral aerosol produced in these two major dust source regions is limited, and this has prevented more quantitative evaluations of source contributions at sites downwind.

* Corresponding author. Tel.: +86 29 88326488; fax: +86 29 88320456.
E-mail addresses: zhangr2002@gmail.com (R. Zhang), cao@loess.llqg.ac.cn (J. Cao).
[1] Permanent address: 28 Quail Meadow Road, Placitas, NM 87043.

0048-9697/$ – see front matter
http://dx.doi.org/10.1016/j.scitotenv.2013.11.011

Schütz and Rahn (1982) were among the first to determine the elemental concentrations of size-separated resuspended soils; these authors analyzed desert soils from Africa and North America. Previous work in Chinese Loess Plateau showed that the chemical profiles for four size factions of particles (total suspended particles or TSP, particulate matter ≤ 10, 2.5 and 1 μm in diameter, PM_{10}, $PM_{2.5}$, and PM_1, respectively) produced from resuspended dust were different and that elemental ratios, such as Ca/Al, Ca/Si, and Ca/Fe, provided information on the sources for Asian dust (Cao et al., 2008). However, comparable information on the chemical composition of fugitive dust produced from the major deserts in China under controlled conditions is only available from a single study by Yuan et al. (2006).

To address this lack of information, our study was designed to characterize the chemical composition and to determine the source profiles of fugitive dust particles produced from sediments collected from six areas typical of the Chinese deserts. The substances analyzed for the study included elements, major ions, organic and elemental carbon, but only the elemental data are discussed here. This is because the other chemical components accounted for less than 10% of the total mass concentration. The elemental data also were used to address a second objective, which was to compare and contrast the elemental composition of particles from the two desert-dust source regions. This dataset will not only be useful for studies of Asian dust (e.g. characteristics and source region identification) but also for quantified source apportionments used in studies of urban air quality (Sun et al., 2004; Huang et al., 2010).

2. Methodology

2.1. Sampling of soils

Much of northern China is covered by deserts and Gobi; these arid and semi-arid lands include the Taklimakan Desert, Gurbantunggut Desert, Kumtag Desert, Qaidam Basin Desert, Badain Jaran Desert, Tengger Desert, Ulan Buh Desert, Kubuqi Desert, Mu Us Desert, and Otingdag Sand Land (Fig. 1). The dry lands in North China are the main sources of Asian dust, and they account for ~55% of the land surface area in Xinjiang Province and large areas in Qinghai, Gansu, Shaanxi, Ningxia, Jilin, Liaoning, Heilongjiang Provinces, and Inner Mongolia. The dust produced in these areas also exerts a profound influence on regional and global climate (Arimoto et al., 2006).

Seventeen sampling sites were chosen to represent six deserts; these sites were selected based on geomorphology and geology; the extent of anthropogenic disturbance; and their contributions to Asian dust production. The sites were in the Taklimakan Desert, Xinjiang Gobi, Anxinan Gobi, Ulan Buh Desert, Central Inner Mongolia Desert, and Erenhot Gobi (Fig. 1, see also Table S1). The total combined sampling area of these desert areas is of the order of 3 million km^2, and representative sampling was conducted by taking into account the surface topography (for example, the windward side or leeward side of sand dunes); this was thought to be the most practical way of collecting samples given the limited resources. Each site was far from anthropogenic interferences, and at all sites a 50 m × 50 m grid was sampled instead of a single point; that is, each sample was a composite of surface soils collected within the sampling area. Surface soils at depths of 1–2 cm were collected with a plastic spatula, and they were stored in sealed plastic bags until they were taken back to the laboratory. Six soil samples were finally obtained by compositing soils from the same desert; they were then dried at 40 °C for 24 h and sieved through Tyler® 30, 50, 100, 200, and 400 mesh sieves (nominal geometric diameter < 38 μm for the 400 mesh sieve).

2.2. Resuspension and chemical analysis

The sieved soil samples were resuspended in a Desert Research Institute particle resuspension system (Chow et al., 1994); then the particles were separated by size aerodynamically and finally collected on Teflon® membrane filters (Whatman $PM_{2.5}$ membranes, Whatman Inc., U.S.A.). For these particle separations, approximately 0.1 mg of sieved material was placed in a 250 ml side-arm vacuum flask. The flask was sealed with a rubber stopper, and the particles were then transferred from the flask into a resuspension chamber by a pulsed-air jet. Clean, filtered, laboratory air was then drawn into the chamber, and the outflow from the chamber was directed through a size separating ($PM_{2.5}$ or PM_{10} or TSP) inlet. The flow rate through the inlets was 5 l min^{-1}.

Before and after sampling, the filters were conditioned at a constant temperature (21.5 ± 0.5 °C) and relative humidity (25 to 30%) and then weighed using a ME 5-F microbalance (Sartorius, Göttingen,

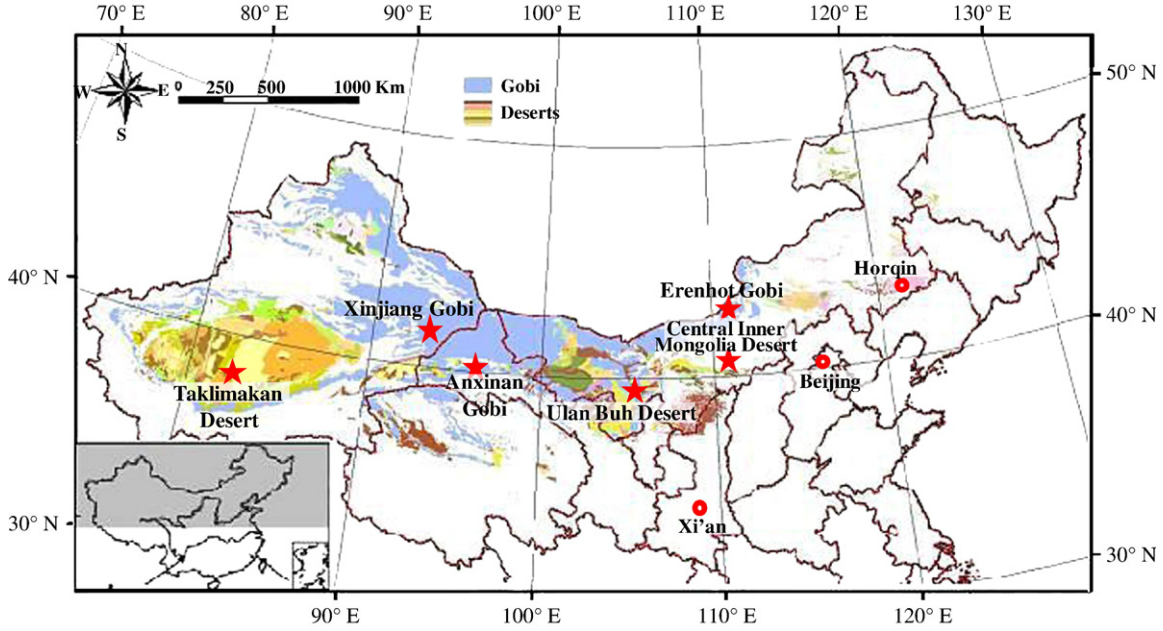

Fig. 1. Fugitive dust sampling sites in the Chinese deserts.

Germany). The sensitivity of the microbalance was ±1 μg; the precisions calculated from two replicate weightings of unexposed and exposed filters were <20 μg and <40 μg, respectively.

Twenty-six elements (Na, Mg, Al, Si, S, Cl, K, Ca, Ti, V, Cr, Mn, Fe, Co, Ni, Cu, Zn, As, Rb, Sr, Mo, Cd, Sn, Sb, Ba, and Pb) were determined with the use of an Energy Dispersive X-ray Fluorescence (EDXRF) (Epsilon 5, PANalytical B. V., the Netherlands). Filter samples were analyzed directly without any preparation procedures (Watson et al., 1999). A three-dimensional polarizing geometry with eleven secondary targets (i.e., CeO_2, CsI, Ag, Mo, Zr, KBr, Ge, Zn, Fe, Ti, and Al) and one barkla target (Al_2O_3) provided a good signal-to-background ratio and low detection limits. The X-ray source was a side window X-ray tube with a gadolinium anode, and it operated at an accelerating voltage of 25–100 kV and a current of 0.5–24 mA (maximum power: 600 W). The ED-XRF spectrometer was calibrated with thin-film standards obtained from MicroMatter Co. (Arlington, WA, USA). The method detection limits (MDLs, μg•cm^{-2}) were Na (1.795), Mg (0.018), Al (0.066), Si (0.374), S (0.006), Cl (0.005), K (0.009), Ca (0.004), Ti (0.003), V (0.002), Cr (0.004), Mn (0.007), Fe (0.016), Co (0.003), Ni (0.003), Cu (0.004), Zn (0.005), As (0.004), Rb (0.004), Sr (0.004),Mo (0.006), Cd(0.030), Sn (0.018), Sb (0.018), Ba (0.051), and Pb(0.012).

To evaluate the effectiveness of this resuspension and collection procedure, the mass of crustal matter was reconstructed by following equation (Chan et al., 1997):

$$\text{Crustal matter} = 1.16 \times [(1.90 \times \text{Al}) + (2.15 \times \text{Si}) + (1.41 \times \text{Ca}) + (1.67 \times \text{Ti}) + (2.09 \times \text{Fe})]. \quad (1)$$

Other components, such as MgO, Na_2O, K_2O, and H_2O, were accounted for by the use of the constant (1.16) in Eq. (1) (Chan et al., 1997). The reconstructed crustal masses of desert soil samples were 76.3% (56.7 to 101%) for TSP, 84.3% (68.2 to 99.9%) for PM_{10}, and 77.5% (56.8 to 86.8%) for $PM_{2.5}$. These results were considered to be reasonable and acceptable because only selected oxides and water were included in the calculations — other compounds, such as sulphate and organic matter, which cannot be neglected in some areas, were neither determined nor taken into account. This is discussed in further detail below.

3. Results and discussion

3.1. Elemental abundances

The elemental profiles for the TSP, PM_{10}, and $PM_{2.5}$ size fractions from six Chinese desert sites were calculated by dividing the concentration of each element by the matching mass concentration; these results are summarized in Tables 1–3. The major dust elements in the desert regions were Si, Al, Fe, Ca, and K: these contributed more than 1% of the total mass for each of the three size fractions. Si was the most abundant element, accounting for 12.5 to 25% of the TSP, 16.6 to 23% of the PM_{10}, and 13 to 23% of the $PM_{2.5}$. Al contents increased in the smaller particle-size fractions, varying from 5.6% (4 to 8%) in TSP to 6.5% (4.5 to 9%) in PM_{10} and 7.4% (5 to 9%) in $PM_{2.5}$. The abundances of Fe were similar in all three size factions from Taklimakan Desert, Xinjiang Gobi, and Anxinan Gobi, but they were much lower at the other three sampling sites, especially in PM_{10} and $PM_{2.5}$ (Tables 2 and 3). The results for K exhibited a pattern similar to Fe. Ca percentages were 2.5 to 6% in TSP, 2 to 7% in PM_{10}, and 1.4 to 4% in $PM_{2.5}$; these values are much lower than what has been reported for Chinese Loess (6.78, 9.83, and 11.2% for TSP, PM_{10}, and $PM_{2.5}$, respectively; Cao et al., 2008). Yuan et al. (2006) reported a relatively high abundance of Ca in fine sand (13.6% for $PM_{2.5}$) from Central Inner Mongolia and an abundance in coarse sand (2.9% for $PM_{2.5-10}$) similar to our results.

The abundance of Mg at Taklimakan Desert, Xinjiang Gobi, and Anxinan Gobi was >1% in all three size fractions, and it was a major species in PM_{10} and $PM_{2.5}$ at Ulan Buh Desert and Erenhot Gobi as well. Na is a major component of Taklimakan soils and also in PM_{10} and $PM_{2.5}$ from the Xinjiang Gobi and Anxinan Gobi. The abundances of S and Cl

Table 1
Summary of fugitive dust elemental profiles (weight percent by mass ± analytical uncertainty) for TSP produced from Chinese desert sediments.

Species	Taklimakan Desert	Xinjiang Gobi	Anxinan Gobi	Ulan Buh Desert	Central Inner Mongolia Desert	Erenhot Gobi	Composite		
							Total [a]	Northwestern [b]	Northern [c]
Na	1.1077 ± 3.3828	0.6889 ± 0.8911	0.7502 ± 0.9643	0.4046 ± 1.5218	0.4117 ± 1.4327	0.3570 ± 0.8825	0.6200	0.8489	0.3911
Mg	2.2820 ± 5.1677	1.1556 ± 0.7757	1.5280 ± 0.8518	0.8197 ± 2.3804	0.7850 ± 2.2230	0.6742 ± 1.2945	1.2074	1.6552	0.7596
Al	7.8752 ± 0.1849	5.7299 ± 0.1067	5.1716 ± 0.0967	3.5561 ± 0.0842	6.5658 ± 0.1306	5.0676 ± 0.0976	5.6610	6.2589	5.0632
Si	25.1321 ± 0.9782	16.3344 ± 0.4808	15.6840 ± 0.4636	12.5314 ± 0.4719	19.5997 ± 0.6328	15.0406 ± 0.4644	17.3870	19.0502	15.7239
S	0.1279 ± 0.0120	0.0887 ± 0.0042	0.1642 ± 0.0075	0.3657 ± 0.0170	0.2025 ± 0.0101	0.1971 ± 0.0091	0.1910	0.1269	0.2551
Cl	0.6029 ± 0.0398	0.2273 ± 0.0147	0.0084 ± 0.0015	0.2031 ± 0.0137	0.0627 ± 0.0056	0.0491 ± 0.0039	0.1923	0.2795	0.1050
K	3.0025 ± 0.0424	2.4663 ± 0.0323	2.3520 ± 0.0308	1.3791 ± 0.0195	2.2070 ± 0.0297	1.8509 ± 0.0245	2.2096	2.6069	1.8123
Ca	3.7100 ± 0.0246	5.2456 ± 0.0336	4.2161 ± 0.0270	5.9178 ± 0.0380	2.5283 ± 0.0164	5.4002 ± 0.0346	4.5030	4.3906	4.6154
Ti	0.4925 ± 0.0125	0.4954 ± 0.0118	0.5064 ± 0.0120	0.3261 ± 0.0080	0.6157 ± 0.0147	0.4688 ± 0.0112	0.4842	0.4981	0.4702
V	0.0053 ± 0.0065	0.0111 ± 0.0105	0.0094 ± 0.0089	0.0089 ± 0.0086	0.0076 ± 0.0074	0.0096 ± 0.0091	0.0087	0.0086	0.0087
Cr	0.0140 ± 0.0082	0.0104 ± 0.0027	0.0087 ± 0.0024	0.0073 ± 0.0039	0.0106 ± 0.0041	0.0039 ± 0.0021	0.0092	0.0110	0.0073
Mn	0.0999 ± 0.0261	0.1161 ± 0.0269	0.1141 ± 0.0264	0.0704 ± 0.0172	0.1080 ± 0.0255	0.0929 ± 0.0217	0.1002	0.1100	0.0904
Fe	5.9521 ± 0.0652	5.6130 ± 0.0557	5.4912 ± 0.0545	3.0194 ± 0.0326	5.6779 ± 0.0574	4.5264 ± 0.0453	5.0467	5.6854	4.4079
Co	0.0105 ± 0.0132	0.0128 ± 0.0151	0.0108 ± 0.0127	0.0040 ± 0.0052	0.0091 ± 0.0109	0.0074 ± 0.0088	0.0091	0.0114	0.0068
Ni	0.0035 ± 0.0060	0.0037 ± 0.0023	0.0047 ± 0.0028	0.0024 ± 0.0030	0.0060 ± 0.0042	0.0022 ± 0.0019	0.0038	0.0040	0.0035
Cu	0.0228 ± 0.0071	0.0059 ± 0.0011	0.0063 ± 0.0012	0.0073 ± 0.0032	0.0068 ± 0.0030	0.0070 ± 0.0018	0.0094	0.0117	0.0070
Zn	0.0315 ± 0.0089	0.0133 ± 0.0020	0.0144 ± 0.0021	0.0178 ± 0.0043	0.0174 ± 0.0041	0.1038 ± 0.0125	0.0330	0.0197	0.0463
As	0.0035 ± 0.0103	0.0017 ± 0.0036	0.0013 ± 0.0028	0.0016 ± 0.0047	0.0008 ± 0.0036	0.0026 ± 0.0055	0.0019	0.0022	0.0017
Rb	0.0000 ± 0.0076	0.0141 ± 0.0145	0.0144 ± 0.0149	0.0008 ± 0.0036	0.0106 ± 0.0114	0.0092 ± 0.0097	0.0098	0.0143	0.0069
Sr	0.1034 ± 0.0223	0.0390 ± 0.0080	0.0294 ± 0.0061	0.0850 ± 0.0177	0.0310 ± 0.0070	0.0701 ± 0.0144	0.0597	0.0573	0.0620
Mo	0.0172 ± 0.0116	0.0194 ± 0.0050	0.0206 ± 0.0053	0.0000 ± 0.0050	0.0074 ± 0.0050	0.0000 ± 0.0027	0.0162	0.0191	0.0074
Cd	0.0228 ± 0.0577	0.0005 ± 0.0073	0.0005 ± 0.0078	0.0089 ± 0.0259	0.0000 ± 0.0224	0.0035 ± 0.0135	0.0072	0.0079	0.0062
Sn	0.0140 ± 0.0320	0.0020 ± 0.0045	0.0031 ± 0.0049	0.0097 ± 0.0150	0.0008 ± 0.0136	0.0035 ± 0.0080	0.0055	0.0064	0.0047
Sb	0.0000 ± 0.0345	0.0040 ± 0.0048	0.0034 ± 0.0050	0.0000 ± 0.0148	0.0234 ± 0.0165	0.0000 ± 0.0080	0.0160	0.0136	0.0234
Ba	0.0841 ± 0.0894	0.0667 ± 0.0161	0.0357 ± 0.0143	0.0097 ± 0.0409	0.0416 ± 0.0387	0.0736 ± 0.0248	0.0519	0.0622	0.0416
Pb	0.0175 ± 0.0230	0.0017 ± 0.0031	0.0008 ± 0.0032	0.0202 ± 0.0135	0.0008 ± 0.0093	0.0083 ± 0.0066	0.0082	0.0067	0.0098

[a] Total: Average of abundances at six sites.
[b] Northwestern: average of abundances at Taklimakan Desert, Xinjiang Gobi, and Anxinan Gobi.
[c] Northern: average of abundances at Ulan Buh Desert, Central Inner Mongolia Desert, and Erenhot Gobi.

Table 2
Summary of fugitive dust elemental profiles (weight percent by mass ± analytical uncertainty) for PM_{10} produced from Chinese desert sediments.

Species	Taklimakan Desert	Xinjiang Gobi	Anxinan Gobi	Ulan Buh Desert	Central Inner Mongolia Desert	Erenhot Gobi	Composite [a]		
							Total	Northwestern	Northern
Na	1.2735 ± 1.7797	0.9540 ± 1.2294	1.3164 ± 1.6303	0.7819 ± 3.8637	0.5749 ± 1.6657	0.5881 ± 1.5135	0.9148	1.1813	0.6483
Mg	1.9756 ± 1.7971	1.3878 ± 1.0430	2.6836 ± 1.2992	1.1780 ± 6.1519	0.6776 ± 2.5135	0.9864 ± 2.2372	1.4815	2.0157	0.9473
Al	8.9156 ± 0.1686	6.5421 ± 0.1224	7.2008 ± 0.1349	4.5541 ± 0.1609	5.5807 ± 0.1170	6.5681 ± 0.1307	6.5602	7.5528	5.5676
Si	20.4229 ± 0.6301	18.0002 ± 0.5351	16.7557 ± 0.5050	23.4198 ± 1.0356	16.5694 ± 0.5758	18.7192 ± 0.6107	18.9812	18.3929	19.5695
S	0.1851 ± 0.0090	0.0947 ± 0.0047	0.2120 ± 0.0097	0.545 ± 0.0273	0.2977 ± 0.0142	0.3506 ± 0.0162	0.2809	0.1639	0.3978
Cl	0.0541 ± 0.0046	0.2430 ± 0.0157	0.0754 ± 0.0052	0.5198 ± 0.0351	0.1525 ± 0.0108	0.1214 ± 0.0087	0.1944	0.1242	0.2646
K	3.8043 ± 0.0500	2.7472 ± 0.0360	3.0925 ± 0.0406	1.8277 ± 0.0306	1.7688 ± 0.0244	2.2144 ± 0.0298	2.5758	3.2147	1.9370
Ca	5.5998 ± 0.0360	6.1264 ± 0.0393	4.1770 ± 0.0268	5.9941 ± 0.0392	2.0507 ± 0.0135	6.1253 ± 0.0394	5.0122	5.3011	4.7234
Ti	0.6391 ± 0.0152	0.5505 ± 0.0131	0.6057 ± 0.0144	0.3333 ± 0.0096	0.4483 ± 0.0108	0.5053 ± 0.0121	0.5137	0.5984	0.4290
V	0.0080 ± 0.077	0.0118 ± 0.0111	0.0131 ± 0.0124	0.0063 ± 0.0077	0.0060 ± 0.0060	0.0129 ± 0.0123	0.0097	0.0110	0.0084
Cr	0.013 ± 0.0040	0.0081 ± 0.0024	0.0112 ± 0.0031	0.0063 ± 0.0091	0.0060 ± 0.0040	0.0053 ± 0.0035	0.0083	0.0108	0.0059
Mn	0.1555 ± 0.0090	0.1321 ± 0.0306	0.1474 ± 0.0342	0.0692 ± 0.0216	0.0907 ± 0.0218	0.1146 ± 0.0270	0.1183	0.1450	0.0915
Fe	7.7847 ± 0.0776	6.1019 ± 0.0606	6.7542 ± 0.0671	3.2694 ± 0.0467	4.2501 ± 0.0442	4.7718 ± 0.0487	5.4887	6.8803	4.0971
Co	0.0142 ± 0.0168	0.0094 ± 0.0111	0.0169 ± 0.0199	0.0042 ± 0.0074	0.0086 ± 0.0104	0.0076 ± 0.0092	0.0102	0.0135	0.0068
Ni	0.0065 ± 0.0042	0.0037 ± 0.0024	0.0065 ± 0.0039	0.0000 ± 0.0068	0.0094 ± 0.0061	0.0046 ± 0.0036	0.0051	0.0056	0.0047
Cu	0.0127 ± 0.0026	0.0078 ± 0.0015	0.0115 ± 0.0019	0.0147 ± 0.0082	0.0103 ± 0.0035	0.0114 ± 0.0031	0.0114	0.0107	0.0121
Zn	0.0263 ± 0.0042	0.0155 ± 0.0024	0.0208 ± 0.0031	0.0314 ± 0.0104	0.0197 ± 0.0046	0.1768 ± 0.0214	0.0484	0.0209	0.0760
As	0.0030 ± 0.0065	0.0020 ± 0.0043	0.0023 ± 0.0049	0.0105 ± 0.0229	0.0009 ± 0.0041	0.0030 ± 0.0068	0.0036	0.0024	0.0048
Rb	0.0210 ± 0.0217	0.0169 ± 0.0174	0.0165 ± 0.0171	0.0000 ± 0.0091	0.0043 ± 0.0058	0.0030 ± 0.0045	0.0103	0.0181	0.0024
Sr	0.0718 ± 0.0148	0.0556 ± 0.0114	0.0269 ± 0.0057	0.2138 ± 0.0445	0.0411 ± 0.0091	0.0819 ± 0.0170	0.0819	0.0514	0.1123
Mo	0.0029 ± 0.0037	0.0000 ± 0.0021	0.0264 ± 0.0069	0.0617 ± 0.0199	0.0252 ± 0.0081	0.0000 ± 0.0047	0.0232	0.0098	0.0435
Cd	0.0024 ± 0.0177	0.0000 ± 0.0100	0.0004 ± 0.0114	0.0105 ± 0.0623	0.0000 ± 0.0254	0.0000 ± 0.0225	0.0044	0.0014	0.0105
Sn	0.0080 ± 0.0110	0.0037 ± 0.0062	0.0000 ± 0.0069	0.0398 ± 0.0404	0.0137 ± 0.0162	0.0015 ± 0.0137	0.0133	0.0059	0.0183
Sb	0.0074 ± 0.0112	0.0013 ± 0.0062	0.0046 ± 0.0073	0.0000 ± 0.0384	0.0000 ± 0.0157	0.0023 ± 0.0139	0.0031	0.0044	0.0012
Ba	0.0639 ± 0.0314	0.0600 ± 0.0193	0.0650 ± 0.0218	0.0482 ± 0.1061	0.0359 ± 0.0435	0.0622 ± 0.0395	0.0559	0.0630	0.0488
Pb	0.0056 ± 0.0077	0.0057 ± 0.0049	0.0062 ± 0.0055	0.0084 ± 0.0261	0.0000 ± 0.0105	0.0159 ± 0.0118	0.0084	0.0058	0.0122

[a] Total, northwestern, and northern as in Table 1.

in $PM_{2.5}$ from soils from the Ulan Buh Desert were 2.45% and 3.2%, respectively. Wu et al. (2012) reported a S abundance of 4% for dust aerosol from Taklimakan Desert, and these authors suggested surface soil as the dominant source for aerosol S. Dry salt-lake saline soils are widely distributed around this area (Zhang et al., 2004), and the high concentrations of S and Cl in the laboratory-produced dust may well have originated from that source.

Trace elements with abundances between 0.1 and 1% included Na (0.6 to 1%), Ti (0.3 to 0.6%), S (0.2 to 0.7%), Cl (0.2 to 0.7%), and Mn (0.09 to 0.1%) in TSP and PM_{10} (Tables 1 and 2). The abundances of Sr, Ba, Zn, Mo, and Sb ranged from 0.01 to 0.1% in TSP, and other elements (Cu, Cr, Co, Rb, Pb, V, Cd, Sn, Ni, and As) were in the range of 0.001 to 0.01%. Four more elements, Cu, Co, Rb, and Sn, showed slightly higher concentrations, ranging from 0.01 to 0.1%, in PM_{10}. The elemental

Table 3
Summary of fugitive dust elemental profiles (weight percent by mass ± analytical uncertainty) for $PM_{2.5}$ produced from Chinese desert sediments.

Species	Taklimakan Desert	Xinjiang Gobi	Anxinan Gobi	Ulan Buh Desert	Central Inner Mongolia Desert	Erenhot Gobi	Composite [a]		
							Total	Northwestern	Northern
Na	1.1236 ± 2.5289	1.2203 ± 1.9126	1.9582 ± 2.8866	0.8953 ± 7.2130	0.2217 ± 4.1534	0.7360 ± 3.9393	1.0259	1.4340	0.6177
Mg	2.3498 ± 3.6248	2.1631 ± 2.2425	4.3174 ± 3.2294	1.2693 ± 11.6694	0.8107 ± 6.7740	1.2617 ± 6.2980	2.0287	2.9434	1.1139
Al	7.5166 ± 0.1598	7.7142 ± 0.1501	7.9887 ± 0.1621	9.0232 ± 0.2713	7.4863 ± 0.1637	5.0936 ± 0.1689	7.4704	7.7398	7.2010
Si	20.3895 ± 0.7454	17.8603 ± 0.5862	18.8377 ± 0.6696	15.0823 ± 1.5001	12.9468 ± 0.8693	23.2818 ± 1.0472	18.0664	19.0292	17.1036
S	0.1246 ± 0.0092	0.1689 ± 0.0088	0.2332 ± 0.0121	2.4451 ± 0.0483	1.0449 ± 0.0295	0.2746 ± 0.0178	0.7152	0.1756	1.2549
Cl	0.0904 ± 0.0086	0.3296 ± 0.0215	0.0558 ± 0.0065	3.2025 ± 0.1310	0.3767 ± 0.0132	0.3648 ± 0.0259	0.7366	0.1586	1.3147
K	2.9981 ± 0.0407	2.8146 ± 0.0374	2.9815 ± 0.0401	2.2689 ± 0.0435	1.4913 ± 0.0263	1.6036 ± 0.0287	2.3597	2.9314	1.7879
Ca	2.9867 ± 0.0197	3.9039 ± 0.0252	2.4766 ± 0.0163	3.7691 ± 0.0246	1.4429 ± 0.0114	4.1379 ± 0.0276	3.1195	3.1224	3.1166
Ti	0.4409 ± 0.0109	0.5157 ± 0.0124	0.4752 ± 0.0116	0.3132 ± 0.0123	0.2509 ± 0.0080	0.3261 ± 0.0095	0.3870	0.4773	0.2967
V	0.0098 ± 0.0097	0.0045 ± 0.0046	0.0110 ± 0.0106	0.0000 ± 0.0095	0.0036 ± 0.0055	0.0000 ± 0.0051	0.0048	0.0084	0.0012
Cr	0.0098 ± 0.0058	0.0097 ± 0.0039	0.0115 ± 0.0053	0.0086 ± 0.0172	0.0099 ± 0.0102	0.0172 ± 0.0101	0.0111	0.0103	0.0119
Mn	0.1111 ± 0.0271	0.1310 ± 0.0307	0.1356 ± 0.0322	0.0758 ± 0.0322	0.0365 ± 0.0193	0.0665 ± 0.0214	0.0928	0.1259	0.0596
Fe	5.6295 ± 0.0590	5.7677 ± 0.0583	5.8146 ± 0.0599	2.9339 ± 0.0696	2.1321 ± 0.0422	2.8753 ± 0.0447	4.1922	5.7373	2.6471
Co	0.0195 ± 0.0232	0.0149 ± 0.0176	0.0151 ± 0.0180	0.0000 ± 0.0103	0.00982 ± 0.0060	0.0000 ± 0.0056	0.0099	0.0165	0.0033
Ni	0.0073 ± 0.0058	0.0037 ± 0.0032	0.0063 ± 0.0050	0.0080 ± 0.0137	0.0069 ± 0.0085	0.0021 ± 0.0071	0.0057	0.0058	0.0057
Cu	0.0159 ± 0.0050	0.0045 ± 0.0029	0.0136 ± 0.0042	0.0318 ± 0.0157	0.0139 ± 0.0090	0.0193 ± 0.0085	0.0165	0.0113	0.0217
Zn	0.0183 ± 0.0061	0.0536 ± 0.0073	0.0235 ± 0.0056	0.0898 ± 0.0210	0.0282 ± 0.0111	0.4055 ± 0.0494	0.1031	0.0318	0.1745
As	0.0049 ± 0.0111	0.0022 ± 0.0055	0.0037 ± 0.0087	0.0159 ± 0.0362	0.0023 ± 0.0110	0.0064 ± 0.0158	0.0059	0.0036	0.0082
Rb	0.0049 ± 0.0073	0.0112 ± 0.0120	0.0104 ± 0.0116	0.0000 ± 0.0173	0.0000 ± 0.0100	0.0000 ± 0.0093	0.0088	0.0088	0.0000
Sr	0.1063 ± 0.0223	0.0342 ± 0.0076	0.0584 ± 0.0126	0.1313 ± 0.0313	0.0092 ± 0.0652	0.1931 ± 0.0404	0.0888	0.0663	0.1112
Mo	0.0040 ± 0.0391	0.0000 ± 0.0046	0.0000 ± 0.0064	0.0109 ± 0.0378	0.0040 ± 0.0265	0.0421 ± 0.0168	0.0153	0.0040	0.0190
Cd	0.0000 ± 0.0362	0.0022 ± 0.0222	0.0000 ± 0.0309	0.0438 ± 0.1275	0.0231 ± 0.0730	0.0172 ± 0.0664	0.0216	0.0022	0.0280
Sn	0.0110 ± 0.0223	0.0000 ± 0.0134	0.0125 ± 0.0193	0.0477 ± 0.0737	0.0167 ± 0.0418	0.0215 ± 0.0394	0.0219	0.0118	0.0286
Sb	0.0000 ± 0.0224	0.0000 ± 0.0136	0.0000 ± 0.0191	0.0159 ± 0.0731	0.0050 ± 0.0423	0.0000 ± 0.0393	0.0105	0.0000	0.0105
Ba	0.0623 ± 0.0624	0.0603 ± 0.0387	0.0876 ± 0.0543	0.0517 ± 0.2011	0.0658 ± 0.1168	0.0494 ± 0.1086	0.0629	0.0701	0.0556
Pb	0.0195 ± 0.0174	0.0000 ± 0.0092	0.0037 ± 0.0129	0.1011 ± 0.0522	0.0194 ± 0.0284	0.0043 ± 0.0265	0.0296	0.0116	0.0416

[a] Total, northwestern, and northern as in Table 1.

abundances in $PM_{2.5}$ varied over several orders-of-magnitude: the mass percentages of Cl, S, Ti, and Zn were in the range of 0.1 to 1%; Mn, Sr, Ba, Pb, Sn, Cu, Cd, Cr, and Mo varied between 0.01 to 0.1% while Co, Rb, V, Ni, As, and Sb ranged from 0.001 to 0.01%. It is worth noting that the abundances of Zn, Cu, Pb, Cd, As, and S, which are often contaminants, were as much as 1.6 to 5 times higher in $PM_{2.5}$ than in the larger particle-size fractions.

3.2. Compositional differences of particles from two Chinese desert regions

The Chinese deserts spread over thousands of kilometers from northwestern to northeastern China; thus one might expect the elemental composition of the desert sediments to vary geographically. Along these lines, Huang et al. (2010) found that the Ca/Al ratio of dust aerosol from the central Taklimakan Desert was quite different from that of Inner Mongolia. Zhang et al. (1996) determined the elemental composition of size-separated aerosols from 12 deserts in China, and they used the chemical data to divide the Chinese deserts into three sources for Asian dusts: the northwestern deserts, northern high-dust deserts, and northern low-dust deserts. Sun et al. (2001) noted that meteorological conditions also are dissimilar among different geographical areas, and these authors identified the Taklimakan Desert in western China and the Gobi regions in Mongolia and northern China as two of the major source regions for Asian dust.

The results of our study, together with the results of prior studies on geographical distributions, show that the Chinese arid and semi-arid lands can be divided into two major source regions: a northwestern (NW) source and a northern (N) source. The northwestern source is represented by the Taklimakan Desert, Xinjiang Gobi, and Anxinan Gobi: there the crustal elements (Si, Al, Fe, Ca and K etc.) are more abundant compared with the northern source. The latter is represented by the Ulan Buh Desert, Central Inner Mongolia Desert, and Erenhot Gobi; at these sites, the pollution elements (Zn, Cu, Pb, Cd, As, and S etc.) were relatively more abundant compared with the NW region.

For the TSP samples, many of the elements were relatively more abundant in the northwestern samples; the exceptions were S, Zn, Sb, and Pb. For these four elements, the respective abundances for the N source samples were 2.0, 2.4, 1.7, and 1.5-fold higher than those in the NW samples. The differences between the NW and N sources are illustrated in Fig. 2. The Mg and Na contents in the samples from the NW source were approximately twice those in the N source samples; this held true for all three size fractions. The differences between pollution element (S, Cl, Zn, Mo, Pb, Cd, Sn, and As; see Section 3.3 for a discussion of trace element sources) concentrations in the NW and N samples were more pronounced in PM_{10} and $PM_{2.5}$ than in TSP, especially in $PM_{2.5}$; the data for these elements are highlighted with red ovals in Fig. 2. Indeed, the concentrations of these elements in the N source samples were 2.0 to 7.5 fold higher in PM_{10} and 1.7 to 12.7 fold higher in $PM_{2.5}$ compared with the NW samples.

Independent-sample T-tests were used to compare the concentrations of each element in the samples from these two sources. Significant differences ($p < 0.05$) were found for Fe, K, Na, Ti, S, Mn, Cr, and Rb in PM_{10} and Fe, K, Ti, Mn, Co, and V in $PM_{2.5}$; however, the differences in crustal elements in TSP were not significant. The greater abundances of pollution elements, especially in the fine-particle mode, imply that anthropogenic emissions have a greater influence on the N source region for Chinese desert dust than the NW one.

3.3. Comparisons with the composition of the upper continental crust

Enrichment factors (EFs) have been commonly used to determine whether crustal or non-crustal sources are mainly responsible for the elemental abundances observed in environmental samples. EFs typically are calculated by normalizing the concentrations of the elements analyzed relative to the composition of the Earth's upper continental crust (UCC); EFs are defined as

$$EF_X = (X/Al)_{sample}/(X/Al)_{crust} \quad (2)$$

where $(X/Al)_{sample}$ represents the concentration ratio of the element of interest to a reference element in a soil or dust sample while $(X/Al)_{crust}$ represents the corresponding ratio in the Earth's UCC (Taylor and McLennan, 1995). Note that we used the UCC as the reference material for the EF calculations because one of the main objectives for the study

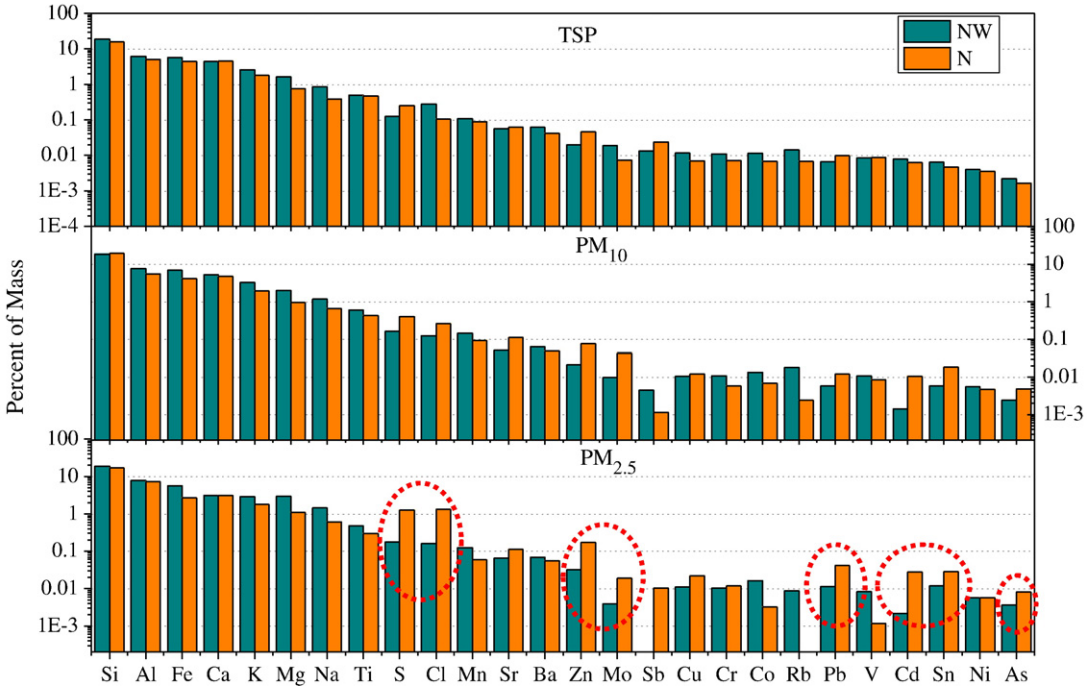

Fig. 2. Chemical components for the northwestern (NW) and the northern (N) composite profiles of TSP, PM_{10}, and $PM_{2.5}$. Dotted circles in red highlight elements with large differences between source regions.

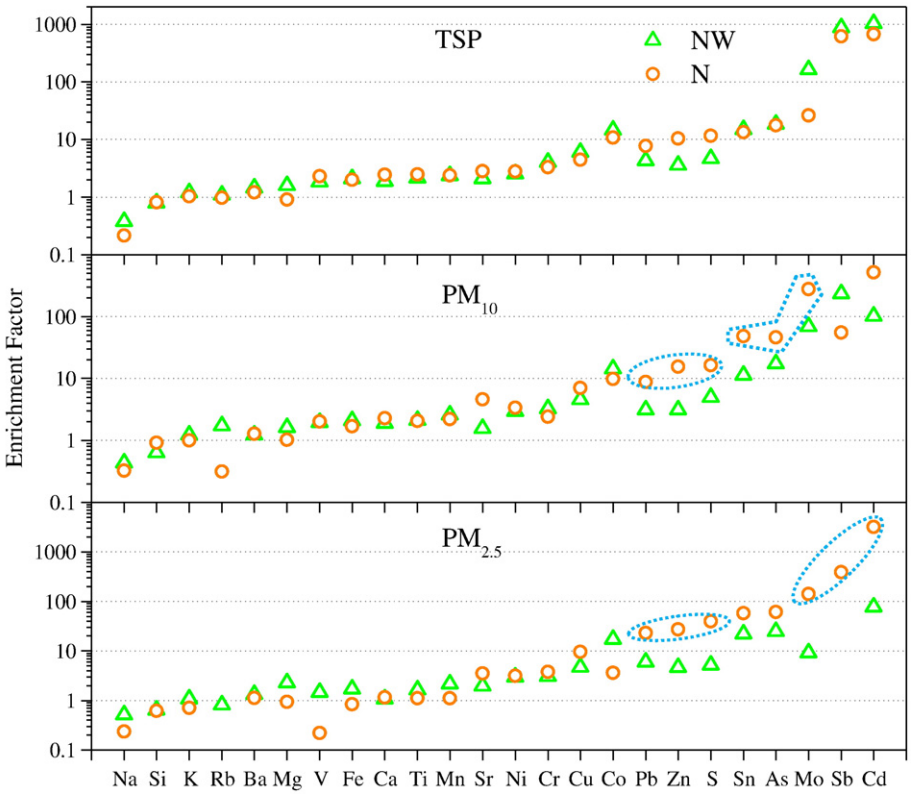

Fig. 3. Elemental enrichment factors relative to UCC (upper continental crust, Taylor and Mclennan, 1995) for TSP, PM_{10}, and $PM_{2.5}$ particles produced from composited desert sediments. Al was used as reference element. Dotted circles in blue highlight elements with larger concentrations in the northern dust source region.

was to compare the composition of the dust from the two dust sources—the use of a single reference material for all sources facilitates such comparisons. Al, a typical crustal element, was used as the reference element in our study.

The EFs for Na, Si, K, Rb, Mg, Ba, V, Fe, Ca, Ti, Mn, Sr, Ni, Cr, and Cu were all lower than 10 in all particle sizes (Fig. 3), and this indicates that the dominant source for these elements was weathered crustal material (Cao et al., 2008). The EFs for Pb, Zn, and S fluctuated above and below 10, which indicates that mixtures of both crustal and non-crustal sources were important for these elements. At the other end of the scale, the EFs for Co, Sn, As, and Mo were in the range of 10 to 100, and the EFs for Sb and Cd ranged from 100 to 1000, implying the dominance of non-crustal sources for these elements even in the desert regions. Of the enriched elements, As, Mo, Sb, and S most likely were enriched as a result of emissions from coal and oil combustion; these fuels are used extensively for both heating and industrial purposes in northern and northwestern China (Hong et al., 2009); Pb was presumably from automotive emissions as well as coal combustion (Xu et al., 2012) while Zn, Cd, and Co were probably discharged from a variety of industrial sources.

The EFs for Pb, Zn, S, Sn, As, Mo, and Cd in both PM_{10} and $PM_{2.5}$ from the N source were higher than those in the NW source while for TSP the EFs for these elements were either similar or the differences relatively small. Therefore, the effects of anthropogenic sources were most pronounced in small particles from the N desert sources. There are numerous coal mines in China located in and around the areas surrounding Inner Mongolia; these include Shizuishan in Ningxia Province, Shenmu in Shaanxi Province, and Datong in Shanxi Province (Aldhous, 2005). One would expect that these coal mines, coking operations, and domestic heating are important, if not dominant, sources for pollutants in neighboring regions.

3.4. Comparisons with aerosol observations

Several studies have investigated the chemical composition of the ambient aerosol in areas affected by dust storms, and we compared our profile data for resuspended $PM_{2.5}$ from the two dust sources with the elemental concentrations of aerosol $PM_{2.5}$ collected during Asian dust storm (DS) episodes. This comparison was done to determine whether the N or NW source materials were more similar to the ambient aerosol data in terms of elemental composition. The aerosol data used for this comparison were from Horqin (located in the center of the Horqin sand land, which is in eastern Inner Mongolia, Shen et al., 2007), Beijing (~700 km from Erenhot, Sun et al., 2005), and Xi'an (the largest city in north central China, this study). As different sets of elements were determined in the various studies, comparisons were necessarily restricted to those elements that were common to the paired data sets of interest.

These comparisons showed that the mass percentages of mineral elements (Al, Ca, Fe, Mn, Si, and Ti etc.) in ambient aerosols collected during dust events in Horqin and Beijing matched those in the N source materials better than the NW ones while the opposite was true for Xi'an. In the spring of 2005, dust originating from the northern sources was transported to Horqin (Shen et al., 2007). As shown in Fig. 4, the abundances of most of the crustal elements, including Si, Al, Fe, K, Mg, Ti, and Mn, in the Horqin samples plotted close to the 1:1 identity line for the N source while the deviations from the 1:1 line were greater when plotted against the NW source. That is, the aerosol data from Horqin matched N source profile much more closely than the NW one. Similarly, at Beijing, the abundances of Al, Fe, Mg, Ti, Mn, and Co in $PM_{2.5}$ from a dust storm that originated to the north in the spring of 2002 (Sun et al., 2005) more closely matched the N source profile. Several points plotted below the 1:1 line in Fig. 4, including several pollution elements (Cu, Pb, and Zn

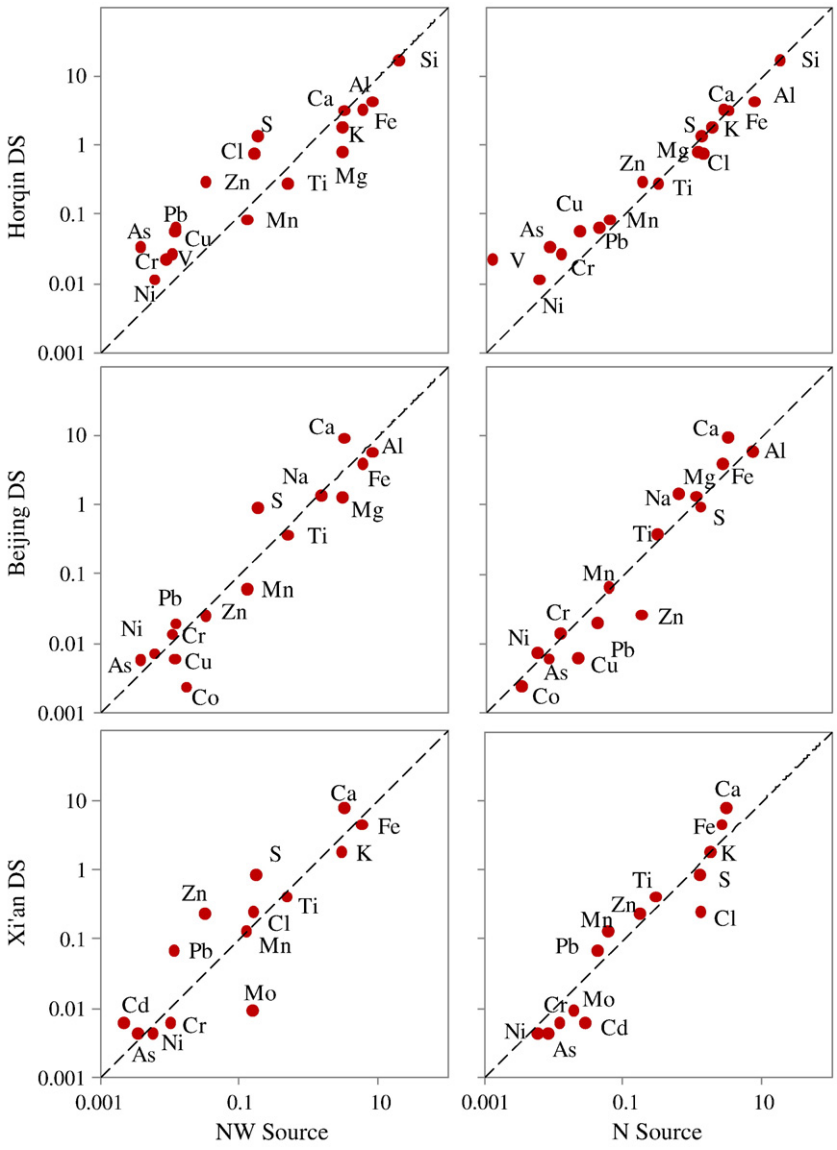

Fig. 4. Comparison of $PM_{2.5}$ chemical components of dust aerosols (DS) produced from the northwestern (NW) and the northern (N) source materials from Chinese deserts.

Table 4
Elemental ratios for resuspended dust from the northwestern (NW) and northern (N) Chinese deserts. Independent-sample T-tests were used to test the differences between sources.

Size	TSP		PM_{10}		$PM_{2.5}$	
Source	NW	N	NW	N	NW	N
Ti/Fe	**0.088 (0.005)**[a,b]	**0.107 (0.003)**	**0.087 (0.005)**	**0.104 (0.002)**	**0.083 (0.006)**	**0.113 (0.006)**
Na/S	*7.00 (2.15)*[c]	*1.65 (0.48)*	*7.72 (2.06)*	*1.68 (0.25)*	**8.21 (0.91)**	**1.09 (1.38)**
Mg/S	*13.4 (4.3)*	*3.18 (0.84)*	**12.7 (2.0)**	**2.42 (0.35)**	**16.7 (3.4)**	**1.96 (2.28)**
Fe/Al	0.93 (0.16)[d]	0.87 (0.02)	**0.91 (0.04)**	**0.74 (0.02)**	*0.74 (0.01)*	*0.39 (0.15)*
K/Al	0.42 (0.04)	0.36 (0.03)	**0.43 (0.00)**	**0.35 (0.04)**	*0.38 (0.02)*	*0.26 (0.06)*
Si/Fe	3.33 (0.77)	3.64 (0.45)	2.68 (0.24)	4.99 (1.88)	*3.32 (0.27)*	*6.44 (1.51)*
Na/Al	*0.14 (0.01)*	*0.08 (0.03)*	0.16 (0.02)	0.12 (0.04)	0.18 (0.05)	0.09 (0.06)
Si/Al	3.02 (0.17)	3.16 (0.32)	2.46 (0.26)	3.65 (1.29)	2.46 (0.22)	2.66 (1.66)
Ca/Al	0.73 (0.23)	1.04 (0.64)	0.71 (0.19)	0.87 (0.48)	0.40 (0.10)	0.47 (0.31)
Mg/Al	0.26 (0.05)	0.16 (0.06)	0.276 (0.09)	0.18 (0.07)	0.38 (0.14)	0.17 (0.07)
Mn/Al	0.018 (0.002)	0.018 (0.006)	0.019 (0.002)	0.016 (0.001)	0.016 (0.001)	0.009 (0.004)
Ti/Ca	0.12 (0.02)	0.13 (0.10)	0.12 (0.03)	0.12 (0.09)	0.16 (0.03)	0.11 (0.05)
S/Fe	0.022 (0.007)	0.067 (0.047)	0.024 (0.008)	0.103 (0.055)	0.031 (0.009)	0.47 (0.37)

[a] Mean (standard deviation).
[b] Bold face type: $p < 0.01$.
[c] Underlined italic type: $p < 0.05$.
[d] Plain text: difference not significant.

etc.); this implies that there were sources for these elements other than deserts of northern China, possibly more distant and relatively cleaner sources in Mongolia, southern Russia or elsewhere.

Xi'an, located in central China, can be influenced by the NW as well as the N dust sources. In comparing the elemental abundances of ambient $PM_{2.5}$ from Xi'an with the two $PM_{2.5}$ source profiles, one can see that the percent contributions of the mineral elements (Fe, Ti, Al, and Mn) to the total mass were more consistent with the NW source. This is reasonable from the standpoint of transport because the prevailing winds during the dust episode were from the west. The obvious differences among the relationships of mineral elements in $PM_{2.5}$ from the three cities with the two different resuspended dust source materials further corroborate the existence of distinct northern and northwestern dust sources.

3.5. Fingerprints of Chinese desert dust sources

Mineral aerosol concentrations have been widely as indicators of air mass movements largely because this material is well characterized chemically, and its composition is relatively stable over time (Zhang et al., 1996). Thus, dust can satisfy two major requirements for a successful regional tracer system, these are: distinctiveness and stability during transport (Lowenthal et al., 1988). Single elements typically cannot serve this purpose for the Chinese deserts or other regions, and therefore elemental ratios, including Si/Fe, Ca/Fe, Si/Al, Fe/Al, Mg/Al, and Sc/Al, have been used as tracers in previous studies. Makra et al. (2002) used the Si/Fe and Ca/Fe ratios to trace the long-range transport of dust from Taklimakan Desert. Zhang et al. (2001) concluded that the ratios of Ca, K, Si, Fe, and Ti to Al could be used as signatures of particles from the Chinese deserts and Loess Plateau; the ratios were then used to estimate the contributions of these sources to aerosol particles from Tibet. The ratios of several crustal to non-crustal elements (Fe/S, Ti/Pb, and Ti/Zn) were reported to be much higher during dust storm events than on non-dusty days in Qingdao (Guo et al., 2004).

Ratios between selected crustal elements (Si, Ca, K, Ti, Al, Fe, and Na) for the resuspended dust and for $PM_{2.5}$ collected on dusty days in previous studies, are listed in Tables 4 and S2. The elemental ratios with statistically significant differences between the NW and N deserts as determined by independent-sample T-tests ($p < 0.05$ and $p < 0.01$) are highlighted in Table 4. All three size fractions showed consistent differences in the Ti/Fe ratios between the NW and N sources, but these differences were only marginally significant. The ratios of Mg/S, Na/S, Na/Al and Mg/Al, in the NW deserts were 1.5 to 8 times those in the N deserts in all particle-size fractions. Differences between sources were observed for the Fe/Al and K/Al ratios in both PM_{10} and $PM_{2.5}$, with relatively higher disparities for $PM_{2.5}$; for that fraction, the NW (N) values for the Fe/Al and K/Al ratios were 0.74 (0.39) and 0.38 (0.26), respectively. Yuan et al. (2006) suggested that the ratios of Mg, K, and Fe to Al (0.47, 0.18, and 1.19, respectively) in $PM_{2.5-10}$ were possible fingerprints of particles from central Inner Mongolia, and those values are quite different from our results (0.18, 0.35, and 0.75 in PM_{10}, and 0.27, 0.37, and 0.60 in $PM_{2.5}$, respectively). In contrast, the Si/Fe and S/Fe ratios in the N source regions were about 2.5 to 7 times those in the NW ones in both PM_{10} and $PM_{2.5}$. The combination of these ratios is therefore potentially useful for distinguishing the two Chinese desert sources.

Along these lines, Sun et al. (2004) used the Mg/Al ratio as a means for distinguishing local versus non-local sources for mineral aerosol in Beijing; for that site, the non-local sources were mainly located in central and eastern Inner Mongolia. Furthermore, the Mg/Al and S/Fe ratios observed in the desert sources were several times higher than the values found for the Chinese Loess Plateau (Cao et al., 2008). The Mg/Al ratios in the NW source were ~4 to 9 times higher those in loess and in the N source 2 to 5 times higher than loess; for S/Fe the differences were 2 to 3 times higher in NW source and 10 to 40 times higher in N source compared with loess.

The Si/Al, K/Al, Ti/Ca, and Ti/Fe ratios for the desert sites were comparable to those of UCC, but the Ca/Al, Fe/Al, Mn/Al, and S/Fe ratios were about twice the UCC values and the Si/Fe ratios were about a half of that in the UCC. Compared with the Chinese Loess Plateau, Ca/Al and Ca/Ti were much lower in desert soils; this is mainly the result of relatively low Ca concentrations in the dust source regions (Cao et al., 2004; Wang et al., 2005). The Si/Al and Ca/Al ratios of dust aerosol from northwestern China (Ta et al., 2003) were similar to the data from our study.

It is worth noting that the ratios of Ca/Al, K/Al, Fe/Al, and Ti/Fe in the Asian dust source regions compared well with those found downwind at Korea, Japan, and the North Pacific (Kim et al., 2003; Arimoto et al, 2006; Ohta et al., 2003). These ratios also differed from those reported for Saharan dusts (Holmes and Miller, 2004; Borbély-Kiss et al., 2004; Remoundaki et al., 2011). Therefore, a combination of these four ratios may be useful as a signature for Asian dust because the ratios are stable during transport and they are distinctly different from mineral aerosol from Africa.

We compared the Fe/Al ratios in the N and NW source materials with those of desert aerosols: Zhang et al. (1996) reported Fe/Al ratios of 0.83, 0.65, and 0.44 in TSP for three desert source regions: I (northwestern), II (high-dust northern), and III (low-dust northern). Consistent with those results, the Fe/Al ratios in the NW source materials were higher than those in the N ones (for $PM_{2.5}$ NW (N) source = 0.74 (0.39); for PM_{10} NW (N) = 0.91 (0.74); for TSP NW (N) = 0.93 (0.87)). Thus, even though the Fe/Al ratios of the TSP dust aerosol in the source areas match our $PM_{2.5}$ source profiles of better than the TSP profiles, the trend of higher Fe/Al ratios in both aerosols and source materials from the NW deserts was consistent between the two studies.

Differences in the elemental ratios as a function of particle size can provide information relative to the strengths of local versus distant sources for dust aerosols. This is because the larger dust particles may be removed from suspension closer to their sources than smaller ones because dry deposition favors the removal of the larger particles. In this regard, the ratios for TSP may be more representative of dust sampled near the sources while the ratios for PM_{10} and $PM_{2.5}$ may be better indicators of the particles that are more susceptible long-range transport.

4. Conclusions

Elemental profiles were determined for size-separated fugitive dust samples produced from sediments collected from six Chinese deserts. The major soil species in the source materials were Si, Al, Fe, Ca, and K; each showed an abundance > 1% in all three (TSP, PM_{10}, and $PM_{2.5}$) size fractions. Dust samples from the N desert soils had relatively lower concentrations of mineral elements (Si, Al, Fe, Ca, K, Mg, Na, and Ti) and higher concentrations of enriched non-crustal elements (S, Zn, Mo, Cu, Cr, Pb, Cd, and As) than the NW ones; these differences were most pronounced in the $PM_{2.5}$ fraction. Enrichment factors (EFs) showed that Cu, Cr, Zn, Pb, As, Mo, and Cd were enriched one to two orders-of-magnitude over the UCC averages, and they were much higher for the northern deserts than the northwestern ones. This implies widespread contamination of the northern deserts, and one important implication of this is that potentially harmful pollutants are likely to be transported together with dust from this source, especially because the enrichments are most pronounced in the finer, more readily transportable particles. Elemental ratios (Na/S, Mg/S, Fe/Al, K/Al, Si/Fe, and Na/Al) are potentially useful tracers that can be used to differentiate the two desert sources. The elemental ratios of Ca/Al, K/Al, Fe/Al, and Ti/Fe in the Chinese desert source materials matched those found in downwind regions, and these ratios may be especially useful for tracing Asian dust.

Conflict of interest

Our manuscript came from our group and we don't have any conflict with other parties.

Acknowledgments

This research was supported in part by the Ministry of Science and Technology (Grants 2013FY112700, 201209007, 2012BAH31B03), the "Strategic Priority Research Program" of the Chinese Academy of Sciences (Grant No. XDA05100401), the National Science Foundation of the United States (ATM0404944), and a grant from the SKLLQG, Chinese Academy of Sciences. The authors wish to thank the staff of the Shaanxi Institute of Desert.

Appendix A. Supplementary data

Supplementary data to this article can be found online at http://dx.doi.org/10.1016/j.scitotenv.2013.11.011.

References

Aldhous P. China's burning ambition. Nature 2005;435:1152–4.
Arimoto R, Kim YJ, Kim YP, Quinn PK, Bates TS, Anderson TL, et al. Characterization of Asian dust during ACE-Asia. Global Planet Change 2006;52:23–56.
Borbély-Kiss I, Kiss ÁZ, Koltay E, Szabó G, Bozó L. Saharan dust episodes in Hungarian aerosol, elemental signatures and transport trajectories. J Aerosol Sci 2004;35:1205–24.
Cao JJ, Lee SC, Zheng XD, et al. Characterization of dust storms to Hong Kong in April 1998. Water Air Soil Pollut 2003;3:213–29.
Cao JJ, Wang YQ, Zhang XY, et al. Analysis of carbon isotope in airborne carbonate: implications for aeolian sources. Chin Sci Bull 2004;49:1637–41.
Cao JJ, Chow JC, Watson JG, Wu F, Han YM, Jin ZD, et al. Size-differentiated source profiles for fugitive dust in the Chinese Loess Plateau. Atmos Environ 2008;42:2261–75.
Cao JJ, Shen ZX, Chow JC, Watson JG, Lee SC, Tie XX, et al. Winter and summer $PM_{2.5}$ chemical compositions in fourteen Chinese cities. J Air Waste Manage Assoc 2012;62:1214–26.
Chan YC, Simpson RW, McTainsh GH, Vowles PD, Cohen DD, Bailey GM. Characterisation of chemical species in $PM_{2.5}$ and PM_{10} aerosols in Brisbane, Australia. Atmos Environ 1997;31:3773–85.
Chio C-P, Cheng M-T, Wang C-F. Source apportionment to PM_{10} in different air quality conditions for Taichung urban and coastal areas, Taiwan. Atmos Environ 2004;38:6893–905.
Chow JC, Watson JG, Houck JE, Pritchett LC, Fred Rogers C, Frazier CA, et al. A laboratory resuspension chamber to measure fugitive dust size distributions and chemical compositions. Atmos Environ 1994;28:3463–81.
Cziczo DJ, Froyd KD, Hoose C, Jensen EJ, Diao MH, Zondlo MA, et al. Clarifying the dominant sources and mechanisms of cirrus cloud formation. Science 2013;340:1320–4.
Guo ZG, Feng JL, Fang M, Chen HY, Lau KH. The elemental and organic characteristics of $PM_{2.5}$ in Asian dust episodes in Qingdao, China, 2002. Atmos Environ 2004;38:909–19.
Holmes CW, Miller R. Atmospherically transported elements and deposition in the Southeastern United States, local or transoceanic? Appl Geochem 2004;19:1189–200.
Hong SL, Hou K, Hur S, Ren SD, Burn J, Rosman LJ, et al. An 800-year record of atmospheric As, Mo, Sn, and Sb in Central Asia in high-altitude ice cores from Mt. Qomolangma (Everest), Himalayas. Environ Sci Technol 2009;43:8060–5.
Huang K, Zhuang GS, Li J, Wang QZ, Sun YL, Lin YF, et al. Mixing of Asian dust with pollution aerosol and the transformation of aerosol components during the dust storm over China in spring 2007. J Geophys Res 2010;115:D00K13.
Kim K-H, Choi G-H, Kang C-H, Lee J-H, Kim JY, Youn YH, et al. The chemical composition of fine and coarse particles in relation with the Asian dust events. Atmos Environ 2003;37:753–65.
Lawrence CR, Neff JC. The contemporary physical and chemical flux of aeolian dust: a synthesis of direct measurements of dust deposition. Chem Geol 2009;267:46–63.
Lowenthal DH, Wunschel KR, Rahn KA. Tests of regional elemental tracers of pollution aerosols. 1. Distinctness of regional signatures, stability during transport, and empirical validation. Environ Sci Technol 1988;22:413–20.
Makra L, Borbély-Kiss I, Koltay E, Chen Y. Enrichment of desert soil elements in Takla Makan dust aerosol. Nucl Instrum Methods Phys Res Sect B 2002;189:214–20.
Martin JH, Fitzwater SE. Iron deficiency limits phytoplankton growth in the north-east Pacific subarctic. Nature 1988;331:341–3.
Ohta A, Terashima S, Kanai Y, Kamioka H, Imai N, Matsuhisa Y, et al. Grain-size distribution and chemical composition of water-insoluble components in aeolian dust collected in Japan in spring 2002. Bull Geol Survey Jpn 2003;54:303–22.
Prospero JM, Ginoux P, Torres O, Nicholson SE, Gill TE. Environmental characterization of global sources of atmospheric soil dust identified with the Nimbus 7 Total Ozone Mapping Spectrometer (TOMS) absorbing aerosol product. Rev Geophys 2002;40:1–31.
Radhi M, Box MA, Box GP, Mitchell RM, Cohen DD, Stelcer E, et al. Size-resolved mass and chemical properties of dust aerosols from Australia's Lake Eyre Basin. Atmos Environ 2010;44:3519–28.
Remoundaki E, Bourliva A, Kokkalis P, Mamouri RE, Papayannis A, Grigoratos T, et al. PM_{10} composition during an intense Saharan dust transport event over Athens (Greece). Sci Total Environ 2011;409:4361–72.
Schütz L, Rahn KA. Trace-element concentrations in erodible soils. Atmos Environ 1982;16:171–6.
Shen ZX, Cao JJ, Arimoto R, Zhang RJ, Jie DM, Liu SX, et al. Chemical composition and source characterization of spring aerosol over Horqin sand land in northeastern China. J Geophys Res 2007;112:D14315.
Sun J, Zhang M, Liu T. Spatial and temporal characteristics of dust storms in China and its surrounding regions, 1960–1999: relations to source area and climate. J Geophys Res 2001;106:10325–33.
Sun Y, Zhuang G, Wang Y, Han L, Guo J, Dan M, et al. The air-borne particulate pollution in Beijing—concentration, composition, distribution and sources. Atmos Environ 2004;38:5991–6004.
Sun YL, Zhuang GS, Wang Y, Zhao XJ, Li J, Wang ZF, et al. Chemical composition of dust storms in Beijing and implications for the mixing of mineral aerosol with pollution aerosol on the pathway. J Geophys Res Atmos 2005;110:D24209.
Sun YB, Tada R, Chen J, Liu QS, Toyoda S, Tani A, et al. Tracing the provenance of fine-grained dust deposited on the central Chinese Loess Plateau. Geophys Res Lett 2008;35:L01804.
Ta W, Xiao Z, Qu J, Yang G, Wang T. Characteristics of dust particles from the desert/Gobi area of northwestern China during dust-storm periods. Environ Geol 2003;43:667–79.
Taylor SR, McLennan SM. The geochemical evolution of the continental crust. Rev Geophys 1995;33:241–65.
Uno I, Eguchi K, Yumimoto K, Takemura T, Shimizu A, Uematsu M, et al. Asian dust transported one full circuit around the globe. Nat Geosci 2009;2:557–60.
Wang YQ, Zhang XY, Arimoto R, Cao JJ, Shen ZX. Characteristics of carbonate content and carbon and oxygen isotopic composition of northern China soil and dust aerosol and its application to tracing dust sources. Atmos Environ 2005;39:2631–42.
Watson JG, Chow JC, Frazier CA. X-ray fluorescence analysis of ambient air samples. In: Landsberger S, Creatchman M, editors. Elemental analysis of airborne particles. New York, NJ: Gordon and Breach Publishers; 1999. p. 67–96.
Wu F, Zhang DZ, Cao JJ, Xu HM, An ZS. Soil-derived sulfate in atmospheric dust particles at Taklimakan desert. Geophys Res Lett 2012;39:L24803.
Xu HM, Cao JJ, Ho KF, Ding H, Han YM, Wang GH, et al. Lead concentrations in fine particulate matter after the phasing out of leaded gasoline in Xi'an, China. Atmos Environ 2012;46:217–24.
Yuan CS, Hai CX, Zhao M. Source profiles and fingerprints of fine and coarse sands resuspended from soils sampled in central Inner Mongolia. China Particuology 2006;4:304–11.
Zhang XY, Zhang GY, Zhu GH, Zhang DE, An ZS, Chen T, et al. Elemental tracers for Chinese source dust. Sci China 1996;39:512–21.
Zhang XY, Arimoto R, An ZS. Dust emission from Chinese desert sources linked to variations in atmospheric circulation. J Geophys Res 1997;102:28041–7.
Zhang XY, Arimoto R, Cao JJ, An ZS, Wang D. Atmospheric dust aerosol over the Tibetan Plateau. J Geophys Res 2001;106:18471–6.
Zhang XY, Zhuang GS, Yuan H. The dried salt-lakes saline soils sources of the dust storm in Beijing — the individual particles analysis and XPS surface structure analysis. China Environ Sci 2004;24:533–7.
Zhuang GS, Yi Z, Duce RA, Brown PR. Link between iron and sulphur cycles suggested by detection of Fe(II) in remote marine aerosols. Nature 1992;355:537–9.